View metadata, citation and similar papers at core.ac.uk

brought to you by CORE

provided by Calhoun, Institutional Archive of the Naval Postgraduate School

Calhoun

Institutional Archive of the Naval Postgraduate School

Calhoun: The NPS Institutional Archive

Faculty and Researcher Publications

Faculty and Researcher Publications

1999

Japan/east Sea (JES) Polar Front meandering and eddy shedding in May 1995.

Chu, Peter C.

Chu, P.C., Y.C. Chen, and S.H. Lu, 1999: Japan/east Sea (JES) Polar Front meandering and eddy shedding in May 1995. International Symposium on Circulation Research of the East

DUDLEY KNOX LIBRARY

http://www.nps.edu/library

Calhoun is a project of the Dudley Knox Library at NPS, furthering the precepts and goals of open government and government transparency. All information contained herein has been approved for release by the NPS Public Affairs Officer.

Dudley Knox Library / Naval Postgraduate School
411 Dyer Road / 1 University Circle
Monterey, California USA 93943

Japan/East Sea (JES) Polar Front Meandering and Eddy Shedding in May 1995

Peter C. Chu
Naval Postgraduate School, Monterey, CA 93943, USA

Yuchun Chen, and Shihua Lu
Institute of Plateau Atmospheric Physics, Academia Sinica, Lanzhou, China

1 Introduction

The Japan Sea, known as the East Sea in Korea, has a steep bottom topography (Figure 1) that makes it a unique semi-enclosed ocean basin overlaid by a pronounced monsoon surface wind. The Japan/East Sea (hereafter JES) covers an area of 10^6 km^2, has a maximum depth in excess of 3,700 m, and is isolated from open oceans except for small (narrow and shallow) straits which connects the JES to the Pacific Ocean. The JES experiences two monsoons, winter and summer, every year. Most analyses on the JES polar front and associated eddies were based on either the sea surface data or limited area data. What is the synoptic structure of the polar front meandering and eddy shedding? What is the sub-surface thermal structure and circulation pattern near the polar front? The Naval Oceanographic Office conducted an intensive airborne expendable bathythermograph (AXBT) survey on 1-8 May 1995 over the majority of the JES down to about 300-m depth. Figure 2 shows the AXBT deployment. This data set provides something close to a 'snapshot' of the temperature in the upper ocean in the JES during the transition time before the onset of the monsoon. Since only temperature-measuring AXBTs were used, no salinity measurements were made at the same time.

2 AXBT Measurements

Most of the 265 AXBTs were deployed at four intervals over a 8-day period from 1 to 8 May 1995. The majority of the AXBTs were nominally capable of reaching a depth of 360-400 m with 1-m vertical resolution. The vertical resolution of the AXBT data is 1 m. Figure 3 shows the ensemble of temperature profiles.

The AXBT observations were mapped to a regular grid using a minimum-curvature spline method with a tension parameter from the Generic Mapping Tools (GMT) [*Smith and Wessel*, 1990; *Wessel and Smith*, 1992]. In order to resolve the mesoscale eddy, we choose $0.25° \times 0.25°$ grid size for the spline function.

3 Inversion of Velocity Field

3.1 Geostrophic Velocity Inverted from Density Field

Recently, *Chu* [1995] and *Chu et al.* [1998b] proposed a simple P-vector inverse method to obtain the absolute velocity from hydrographic data. A velocity vector is represented into a product of a unit vector (P-vector) and a scalar,

$$\mathbf{V} = r(x, y, z)\mathbf{P}. \tag{1}$$

The inversion of $\mathbf{V}$ is fulfilled by two steps: (1) determination of the unit vector $\mathbf{P}$, and (2) determination of the scalar $r(x, y, z)$. Since the geostrophic flow is along both the isopycnal and the iso-potential vorticity surfaces, the velocity $\mathbf{V}$ is parallel to $\nabla q \times \nabla \rho$. Here, ρ is the potential density, and $q = f\partial\rho/\partial z$, is the potential vorticity. If the ρ surface is not parallel to the q surface, the unit vector $\mathbf{P}$ can be defined by [*Chu*, 1995]

$$\mathbf{P} = \frac{\nabla\rho \times \nabla q}{|\nabla\rho \times \nabla q|} \tag{2}$$

Chu et al. [1998b] shows advantages of using the P-vector method. A least square error algorithm [*Chu et al.*, 1998b] is used to minimize the error. For further details and validation of the algorithm presented here see *Chu et al.* [1998c]. Interested readers can obtain the software by contacting Mr. Chenwu Fan at fan@nps.navy.mil.

4 Results

4.1 Thermal Field

4.1.1 Horizontal Structure

Figures 4a-e are horizontal depictions of temperature at 0-, 50-, 100-, 200-, and 300-m depths, respectively.

The contour interval is 0.5°C. In them we see the Polar Front occurring near 40°N with meandering and stretching from the east Korea Bay (EKB) to Tsugaru Kaikyo (TK). Its strength increases from the surface (Figure 4a) to 100 m depth (Figure 4b,c) and then decreases below that depth. The maximum horizontal temperature gradient of the Polar Front is around 8°C/100 km, appearing near EKB at 100 m depth (Figure 4d). At 200 m (Figure 4e) and 300 m (Figure 4f) depths, the Polar Front is broken into several eddies. The Polar Front separates the cold water entering the JES from the north (Sea of Okhotsk) and the warm water entering the JES from the south (Yellow Sea) through the Korea Strait. The thermal features of these eddies are listed in Table 1.

4.1.2 Vertical Structures

Three zonal cross-sections (43°N, 39°N, and 36°N) of temperature show the vertical structure of the mixed layer and the thermocline in the north of, along, and in the south of the Polar Front, respectively (Figure 5). Below 300 m depth, the temperature is uniformly cold (2°C) at all three cross-sections, which confirms the existence the JES Proper Water.

The 39°N cross-section clearly shows the existence of three warm-core eddies near 131°E, 133°E, and 137°30'E from the downward bending (trough) of isotherms. The longitudinal span of the three warm eddies (NKS, OG, and YB) is around 200 km. The 36°N cross-section clearly shows the downward bending (trough) of isotherms between 130°30'E and 132°30'E, indicating the existence of a warm-core eddy. Both 39°N and 36°N cross-sections clearly shows the upward bending (ridge) of isotherms between 131°E and 133°E, indicating the existence of a cold-core eddy, the TB eddy.

4.2 The JES Circulation

The P-vector method [*Chu*, 1995; 1998b,c] was used to determine the velocity field from hydrographic data. Since there were no salinity (S) observations in JES during 1-8 May 1995, May climatological salinity [*Levitus et al.*, 1994] were interpolated to the AXBT stations and those salinity values ($\overline{S}$) were used for the P-vector computation.

The inverted velocity field (Figure 6) indicates the evident Polar Front meandering and eddy shedding. It is easy to identify three warm-core (Figure 4) baroclinic eddies: North Korea Strait (NKS) eddy, Oki Gunto (OG) eddy, and Yamaton Basin (YB) eddy. These eddies are anticyclonic at upper levels (0, 50, and 100 m), and cyclonic at lower level (300 m). It is easy to identify the Tsushima Basin (TB) cold-core cyclonic eddy. The kinetic features of these eddies are listed in Table 1.

4.2.1 Zonal Cross Sections of v-Component

Three zonal cross-sections (43°N, 39°N, and 36°N) of v-velocity show the vertical eddy structure (Figure 7). The positive values indicate northward velocity, and the negative values refer to the southward velocity. Alternate positive and negative areas indicate the occurrence of cyclonic and anticyclonic eddies. At each zonal cross-section, neighboring eastern negative/ western positive patterns refer to an anticyclonic eddy. Neighboring western negative/ eastern positive patterns refer to a cyclonic eddy. There is no evident eddy structure in 43°N cross-section.

The 39°N cross-section clearly shows the existence of the NKS, OG, and YB eddies with high baroclinicity: anticyclonic above 200 m depth and cyclonic below 200 m depth. The three eddies reveal a slightly asymmetric feature. The northward velocity in the western part is a little stronger than the southward velocity in the eastern part. For example, the YB warm-core eddy has a maximum northward speed of 9 cm/s in the western part and a maximum southward speed of 4 cm/s in the eastern part.

The 36°N cross-section clearly shows the co-existence of the NKS warm-core eddy and the TB cold-core eddy sharing a wide southward branch between 130°E and 132°E. The zonal span of both eddies is around 200 km. The depth of the NKS warm-core eddy is around 400 m with anticyclonic tangential velocity above 200 m depth and cyclonic below 200 m depth. The depth of the TB cold-core eddy is quite shallow (above 200 m depth). Both eddies are quite asymmetric with a maximum tangential velocity of 5 cm/s at the southward branch.

4.3 Mechanisms

In searching for mechanisms for the JES Polar Front meandering and eddy shedding, *Chu et al.* [1998a] found a high correlation between surface wind stress curl and sea surface temperature (SST) anomaly with one month lead of wind from correlation analysis of the European Center for Medium-range Weather Forecast (ECMWF) analyzed wind stress data and the National Centers for Environmental Prediction (NCEP) SST data. The high correlation leads to a hypothesis for the wind-driven JES Polar Front meandering and eddy shedding. We will use a numerical model to test this hypothesis.

5 Conclusions

1) Minimum curvature cubic spline analysis of the AXBT data allowed us to identify the JES Polar Front meandering and eddy shedding during 1-8 May 1995. The maximum horizontal temperature gradient of the Polar Front is around 8°C/100 km, appearing near EKB at 100

m depth. The meandering strengthens with depth from the surface to 100 m depth. The northward meandering of the Polar Front at 131°E, 134°E, and 137°E forms several warm-core eddies. The southward meandering of the Polar Front at 132°E forms a cold-core eddy. Three major warm-core eddies were shed from the Polar Front: NKS eddy, OG eddy, and YB eddy. A weak cold-core TB eddy was also identified.

2) The three warm-core eddies have comparable sizes (200 km). They are highly baroclinic with anticyclonic rotation (maximum speed around 10 cm/s) above 200 m depth and cyclonic rotation (maximum speed around 4 cm/s) below 200 m depth.

3) The TB cold-core eddy is quite weak and shallow (above 200 m depth). The maximum tangential velocity is around 6 cm/s.

4) The wind-driven mechanism for the JES Polar Front meandering and eddy shedding during the spring-to-summer transition was confirmed by a numerical study. A manuscript on this modeling study was prepared for submission.

6 Acknowledgments

This work was funded by the Naval Oceanographic Office, the Office of Naval Research (ONR) Naval Ocean Modeling and Prediction (NOMP) Program, and the Naval Postgraduate School.

References

Chu, P.C.,P-vector method for determining absolute velocity from hydrographic data. *Mar. Tech. Soc. J.*, 29 (3), 3-14, 1995.

Chu, P.C., Y.C. Chen, and S.H. Lu, Temporal and spatial variabilities of Japan Sea surface temperature and atmospheric forcing. *J. Oceanogr.*, **54**, in press, 1998a.

Chu, P.C., C.W. Fan, and W.J. Cai, Evaluation of P-vector method using modular ocean model (MOM). *J. Oceanogr.*, **54**, 185-198, 1998b.

Chu, P.C., C.W. Fan, C.J. Lozano, and J.L. Kerling, An airborne expandable bathythermograph survey of the South China Sea, May 1995. *J. Geophys. Res.*, **103**, 21637-21652, 1998c.

Isoda, Y., S. Saitoh, and M. Mihara, Sea surface temperature structure of the polar front in the Japan Sea. *Oceanography of Asian Marginal Seas*, edited by K. Takano, Elsevier, New York, 103-112, 1991.

Katoh, O., Structure of the Tsushima Current in the southwestern Japan Sea. *J. Oceanogr.*, **50**, 317-338, 1994.

Table 1. Locations, Typical Temperatures, and Tangential Velocities of Major JES Polar Front Shaded Eddies Appearing During May 1-8, 1995

Depth (m)	0	50	100	200	300
NKS warm-core eddy	129°-131°E 35°-37°N 16°C, 10 cm/s Anticyclonic	129°-132°E 36°-38°N 13°C, 8 cm/s Anticyclonic	129°-131°E 36°-38°N 11°C, 5 cm/s Anticyclonic	129°-132°E 36°-38°N 6°C, 3 cm/s Cyclonic	129°-132°E 36°-38°N 2°C, 4 cm/s Cyclonic
Oki Gunto warm-core eddy	133°-134°E 36°-39°N 13°C, 6 cm/s Meandering	133°-135°E 36°-39°N 12°C, 8 cm/s Anticyclonic	133°-135°E 36°-39°N 9°C, 5 cm/s Anticyclonic	133°-135°E 36°-39°N 7°C, 2 cm/s Cyclonic	133°-135°E 36°-39°N 2°C, 4 cm/s Cyclonic
YB warm-core eddy	135°-137°E 38°-40°N 13°C, 10 cm/s Meandering	136°-138°E 38°-40°N 10°C, 8 cm/s Anticyclonic	136°-138°E 38°-40°N 10°C, 5 cm/s Anticyclonic	136°-138°E 38°-40°N 6°C, 2 cm/s Cyclonic	136°-138°E 38°-40°N 4°C, 4 cm/s Cyclonic
TB cool-core eddy	131°-131°E 36°-38°N 13°C, 6 cm/s Cyclonic	131°-133°E 36°-38°N 10°C, 6 cm/s Cyclonic	131°-133°E 36°-38°N 6°C, 5 cm/s Cyclonic	131°-133°E 36°-38°N 3°C, 2 cm/s Cyclonic	131°-133°E 36°-38°N 2°C, 1 cm/s Cyclonic

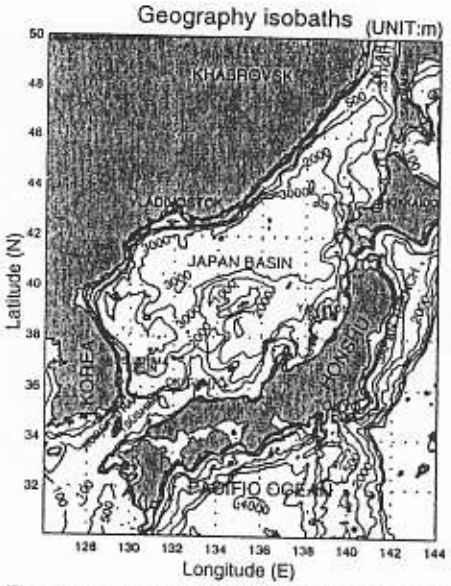

Fig. 1. Geography and isobaths showing the bottom topography of the Japan/East Sea.

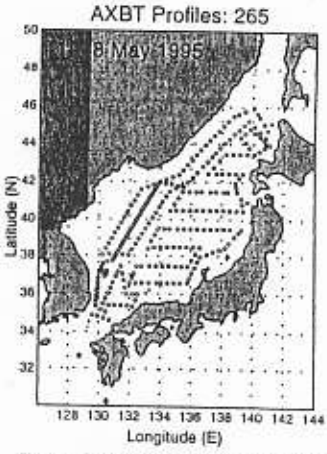

Fig.2 Deployment pattern of AXBT survey during 1–8 May 1995

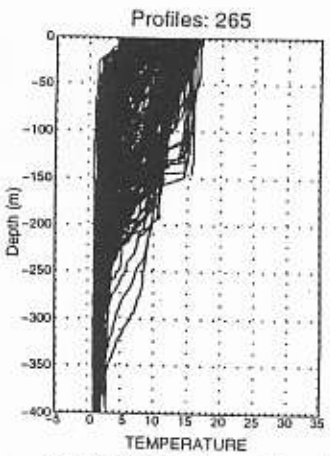

Fig. 3. Temperature profiles of AXBT survey during 1–8 May 1995

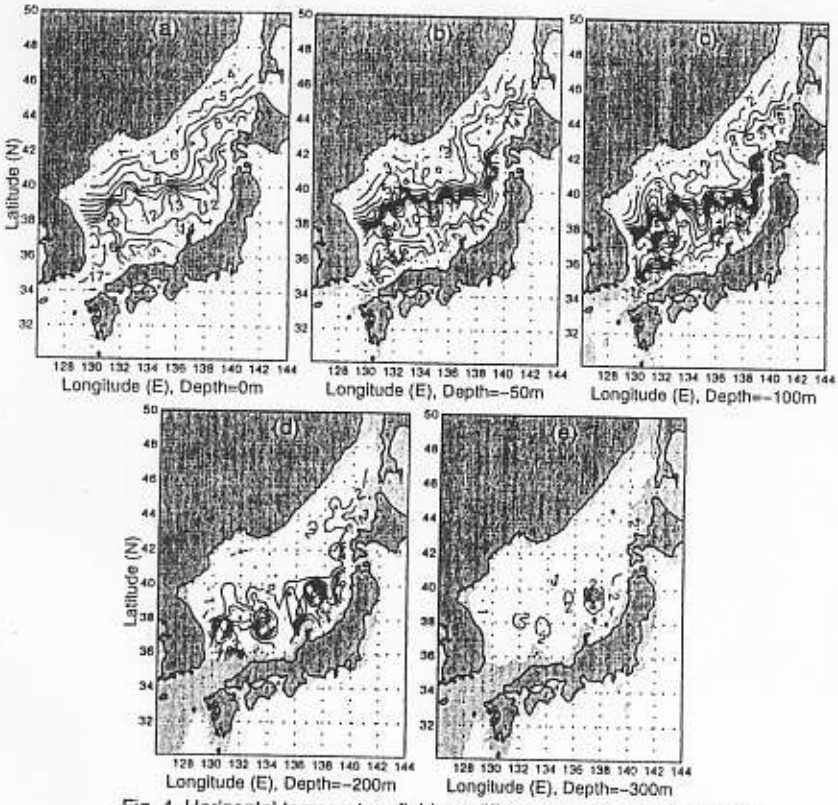

Fig. 4. Horizontal temperature fields at different depths: (a) 0m, (b) 50m, (c) 100m, (d) 200m, and (e) 300m. The Polar Front with meandering and eddy shedding is clearly seen from the surface to 100m depth

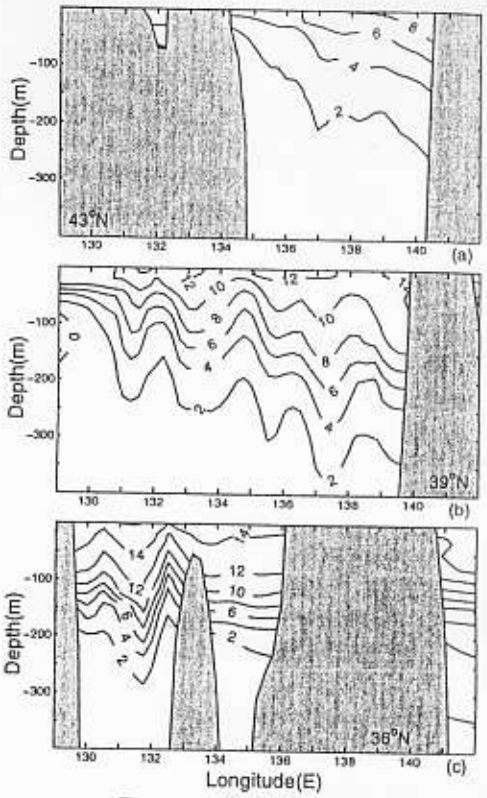

Fig.5 Temperature distribution at several zonal cross section

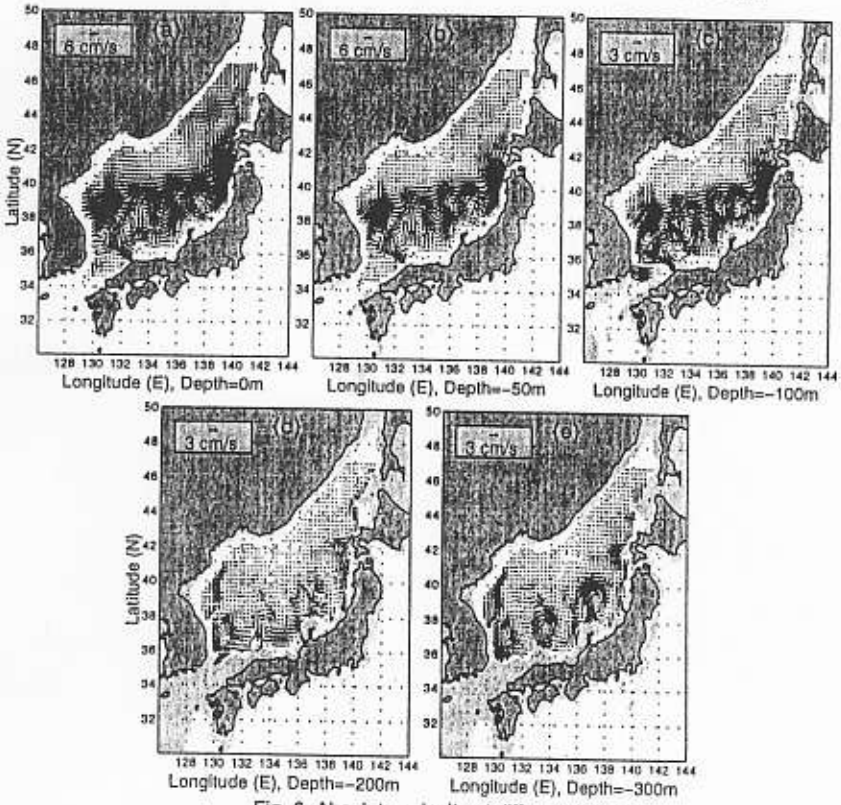

Fig. 6. Absolute velocity at different depths: (a) 0m, (b) 50m, (c) 100m, (d) 200m, and (e) 300m

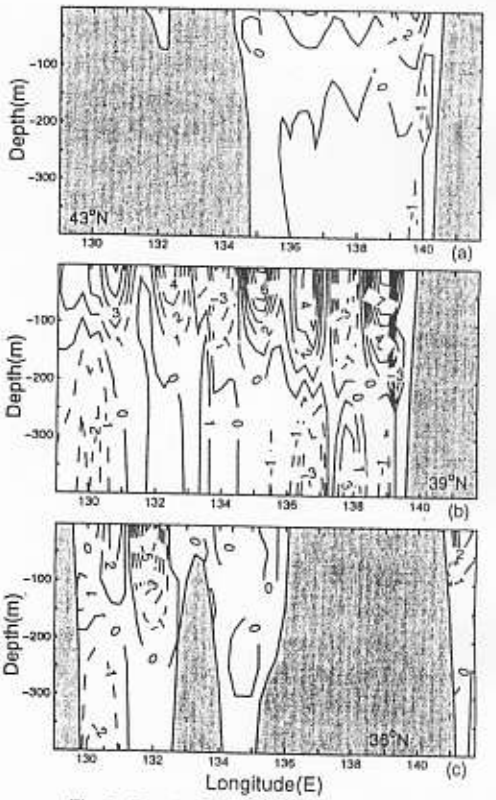

Fig. 7. Distribution of velocity v-component at several zonal cross section